THE GEOLOGICAL SOCIETY OF AMERICA®

Complementary crystal accumulation and rhyolite melt segregation in a late Miocene Andean pluton

Allen J. Schaen[1], John M. Cottle[2], Brad S. Singer[1], C. Brenhin Keller[3,4], Nicolas Garibaldi[1], and Blair Schoene[3]
[1]Department of Geoscience, University of Wisconsin–Madison, Madison, Wisconsin 53706, USA
[2]Department of Earth Science, University of California, Santa Barbara, California 93106, USA
[3]Department of Geosciences, Princeton University, Princeton, New Jersey 08544, USA
[4]Berkeley Geochronology Center, 2455 Ridge Road, Berkeley, California 94709, USA

ABSTRACT

High-silica granites are hypothesized to form via fractionation in the shallow crust, yet the predicted residues are rarely identified and can be difficult to distinguish within plutons whose rocks otherwise plot along liquid lines of descent. Bulk-rock compositional mass balance in the late Miocene Risco Bayo–Huemul plutonic complex (Chile) suggests that lithological differences within the Huemul pluton reflect residual crystal concentration in response to melt extraction. A compositional gap from 70 to 75 wt% SiO_2 and strong depletion in Ba and Eu suggest that Huemul alkali feldspar (Afs) granites are frozen remnants of highly evolved rhyolitic melt extracted from a mush. Quartz monzonites enriched in Zr and Ba with Eu/Eu* near unity are interpreted to represent the complementary residual silicic cumulates of this fractionation process. Compositional variations in Afs granite zircon (Eu/Eu*, Dy/Yb) further support extraction of this melt from a zircon-saturated mush. U-Pb zircon dates indicate that Huemul rocks evolved ~800 k.y. after initial crystallization of more mafic Risco Bayo rocks, likely precluding their evolution via fractionation from mafic forerunners. This pluton records a means to produce rhyolite in the upper crust, which has propelled large silicic eruptions during the Quaternary within the Andean subduction zone.

INTRODUCTION

Processes responsible for generating high-silica granite and rhyolite have important implications for the geochemical evolution of magmas within continental crust and understanding the relationship between plutonic and volcanic rocks (e.g., Bachmann and Huber, 2016; Lundstrom and Glazner, 2016). High-silica (>70 wt% SiO_2) compositions are widely hypothesized to form via crystal-liquid segregation (i.e., fractionation) of interstitial melt from upper crustal, crystal-rich mush systems (Hildreth, 2004; Bachmann and Bergantz, 2004; Gualda and Ghiorso, 2014). Such a model suggests an important role for shallow differentiation in generating silicic magmas and necessitates formation of a corresponding cumulate residue in the middle to upper crust concurrent with melt segregation (e.g., Deering and Bachmann, 2010; Gelman et al., 2014; Lee and Morton, 2015). This model implies that plutonic rocks are genetically related to volcanic products and, in some cases, are interpreted to be the residual material left behind after caldera-forming eruptions (e.g., Deering et al., 2016). However, evidence against general application of this model includes the observation that cumulate lithologies are not readily apparent in global whole-rock geochemical compilations (Glazner et al., 2015).

Here we present geochemical and geochronological evidence that high-silica leucogranites were segregated from their complementary silicic residues during upper crustal fractionation, and both were preserved within the epizonal Risco Bayo–Huemul (RBH) plutonic complex, Chile (Fig. 1). Laser ablation–split stream–mass spectrometry (LASS; Kylander-Clark et al., 2013) on zircon within each magmatic domain supports inferences based on bulk-rock compositions, and places melt compositions in a temporal framework. Whereas others have suggested the presence of silicic cumulates in extensional environments (e.g., Bachl et al., 2001) and larger scale batholiths (Lee and Morton, 2015), we document an example within the archetype continental arc of the Southern Andes. This plutonic record emphasizes the role of upper crustal crystal-liquid segregation in generating silicic cumulate rocks and highlights that high-silica granite is the intrusive equivalent to rhyolite, bolstering the connection between the volcanic and plutonic realms.

RBH PLUTONIC COMPLEX

The late Miocene RBH plutonic complex is located within the southern volcanic zone of the Andes (Fig. 1) and intrudes Oligocene to Miocene metavolcanic rocks (Drake, 1976). Quaternary glaciation and rapid uplift have exposed ~1500 m of the roof zone, and Al-in-hornblende barometry suggests emplacement at 3.7–4.4 km depth (Nelson et al., 1999). Based on new geologic mapping, as well as compositional, textural, and zircon age and chemical variations, distinct magmatic domains within each pluton are defined (Fig. 1; see the GSA

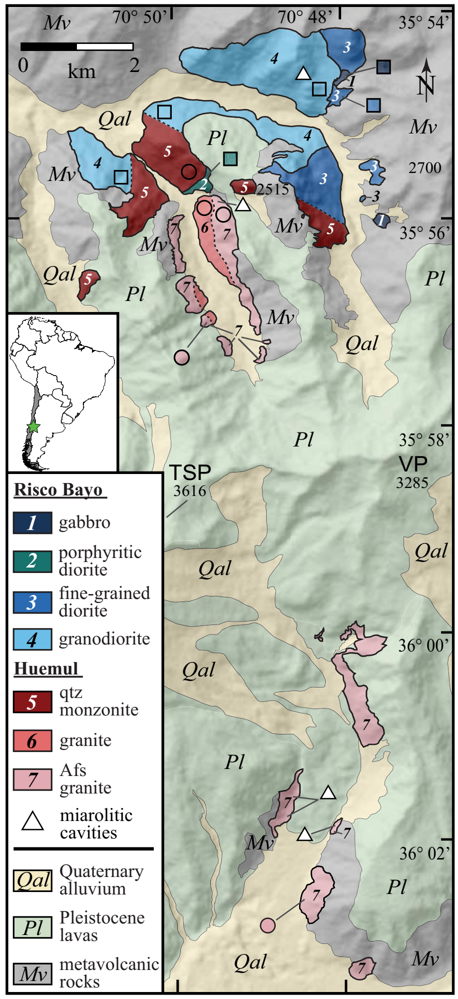

Figure 1. Map of Risco Bayo–Huemul plutonic complex (Chile) highlighting compositional domains of this study (modified from Singer et al., 1997; Nelson et al., 1999). Solid lines are sharp contacts; dashed lines are gradational. Squares and circles are laser ablation–split stream–mass spectrometry sample localities. TSP—Tatara–San Pedro volcano; VP—Pellado volcano; qtz—quartz; Afs—alkali feldspar. Spot elevations are in meters.

GEOLOGY, September 2017; v. 45; no. 9; p. 835–838 | Data Repository item 2017280 | doi:10.1130/G39167.1 | Published online 10 July 2017

Data Repository[1]). Magmatic domains of the more mafic Risco Bayo pluton, each separated by sharp contacts, include gabbro, porphyritic diorite, fine-grained diorite, and granodiorite. In contrast, the adjacent Huemul pluton is leucocratic and comprises three domains, granite, alkali feldspar (Afs) granite, and quartz monzonite, separated by gradational contacts. The granite domain underlies the laterally continuous Afs granite in all northern outcrops but does not crop out in the south (Fig. 1). We interpret these field constraints to reflect layering at depth (see the Data Repository). A ~2000 m^2 zone comprising ~10 vol% of centimeter-diameter miarolitic cavities lined with euhedral quartz, orthoclase, and tourmaline (Fig. 1; see the Data Repository) attests to epizonal emplacement (e.g., Candela, 1997) and volatile saturation of the Huemul Afs granite melt.

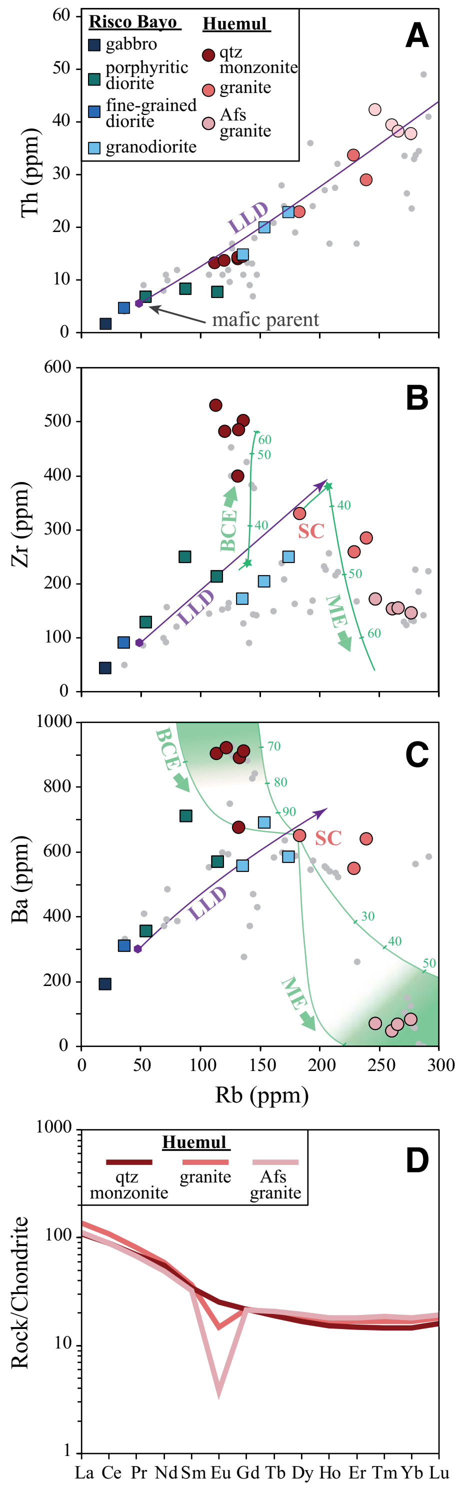

Figure 2. Whole-rock trace element compositions. Melt evolution via fractional crystallization of mafic parent without zircon or K-feldspar (liquid lines of descent, LLD) (qtz—quartz; Afs—alkali feldspar). Complementary fractional crystallization models use the same granitic starting composition (SC) tracking evolution of melt (ME), and the bulk cumulate crystallized from that melt (BCE). A: Th versus Rb. B: Zr versus Rb. Plot illustrates Zr evolution via zircon saturation; green stars indicate common points of zircon saturation. C: Ba versus Rb. Plot uses a range of published end-member solid-melt partition coefficients to create bracketing models (bulk D = 2.5–8). Green fields indicate optimal crystallinity window for melt extraction. Tick marks indicate crystallinity percent. Previously measured Risco Bayo–Huemul (Chile) rocks (small gray circles) are from Nelson et al. (1999). D: Rare earth element patterns of average whole-rock compositions in the Huemul pluton. Details are provided in the Data Repository (see footnote 1).

Huemul rocks comprise orthoclase, plagioclase, quartz, biotite, amphibole, magnetite, apatite, zircon, and rare titanite. Amphibole is present in both the quartz monzonite and granite domains (5–15 modal%), but not in the Afs granite; biotite is present in all Huemul domains. Quartz is typically anhedral and/or interstitial and myrmekitic to micrographic within the zone of miarolitic cavities; orthoclase displays variable perthitic textures in the Afs granite. The Huemul quartz monzonites are of particular interest because they have medium-grained porphyritic textures, including interstitial anhedral quartz and Afs within partially interlocking euhedral plagioclase phenocrysts. The two-stage crystallization implied by these porphyritic textures is inferred to represent residual crystal concentration in response to melt segregation. Cumulate textures are well known in layered mafic intrusions and easily identified in what are typically unimodal rocks (e.g., Wager and Brown, 1968). Concentration of crystals in rarely unimodal granitoids is less commonly recognized, perhaps due to slow rates of crystal growth and transport of higher viscosity melts (e.g., Vernon and Collins, 2011; Lee and Morton, 2015). Here we distinguish between mafic and silicic cumulates and suggest that absence of true adcumulate and orthocumulate textures in the quartz monzonites reflects the concentration of crystals via expulsion of melt from a compacting crystal-rich mush (Bachmann and Bergantz, 2004).

IDENTIFYING SILICIC CUMULATES AND EXTRACTED RHYOLITIC LIQUIDS

Terminal porosity calculations suggest that inefficient melt extraction from an upper crustal granitic mush is likely to leave significant proportions (>20%–30%) of trapped rhyolitic melt, partially to completely concealing geochemical signatures of crystal concentration (Lee and Morton, 2015). Consequently, the residues of melt extraction (silicic cumulates) can be difficult to detect geochemically. However, their presence has been inferred from variations in highly incompatible trace elements (Lee and Morton, 2015) as well as elements that shift from incompatible to compatible behavior during differentiation (e.g., Ba, Zr; Deering and Bachmann, 2010). The degree of melt extraction should be an important control on whether silicic cumulates exhibit compositions that deviate from liquid lines of descent (LLD) and has been suggested as a major reason for their elusiveness in the plutonic rock record (Deering and Bachmann, 2010; Gelman et al., 2014; Lee and Morton, 2015).

We use these criteria and the behavior of Zr and Ba to highlight an example of crystal concentration via compaction and extraction of rhyolitic melt in the Huemul pluton. Zr and Ba are incompatible in mafic melt, and increase in concentration to granodioritic compositions until zircon and alkali feldspar (±biotite) crystallize (Fig. 2). While compositional variation of the entire suite is matched by a singular LLD in Th-Rb space (Fig. 2A), such a model cannot generate the quartz monzonites in Zr-Rb or Ba-Rb space (Figs. 2B and 2C) without unreasonably varying the mineral assemblage or partition coefficients. Observed enrichments of Zr (>400 ppm) and Ba (≥900 ppm) in quartz monzonites require a process other than differentiation of mafic to intermediate liquids. Crustal melting resulting in a high Zr-Ba end member is not easily justified given the low Rb contents of the quartz monzonites and their shallow emplacement histories within the cold upper crust.

The high-silica (~76 wt% SiO_2) Afs granites display strong depletions in Ba and Eu typical of rhyolitic liquids (Figs. 2C and 2D; e.g., Hildreth, 2004). It is hypothesized that these features, together with the enriched bulk composition of the quartz monzonites, are related. We model unmixing of an initially granitic magma and track the complementary trajectories of expelled melt and the residual crystal cumulate (Figs. 2B and 2C). These models produce Afs granites as evolved liquids and suggest that quartz monzonites are not liquid compositions, but concentrates of zircon and feldspar (±biotite)

[1]GSA Data Repository item 2017280, LASS/whole-rock data, methods, field relationships/cross section, model details, QAP ternary, and zircon CL images, is available online at http://www.geosociety.org/datarepository/2017/ or on request from editing@geosociety.org.

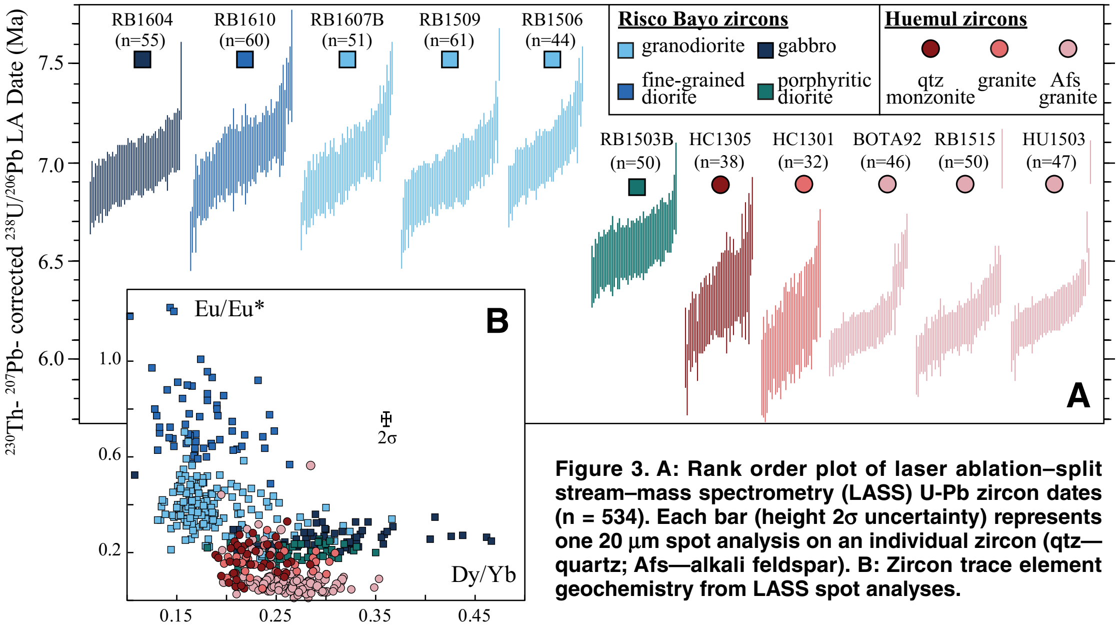

Figure 3. A: Rank order plot of laser ablation–split stream–mass spectrometry (LASS) U-Pb zircon dates (n = 534). Each bar (height 2σ uncertainty) represents one 20 µm spot analysis on an individual zircon (qtz—quartz; Afs—alkali feldspar). B: Zircon trace element geochemistry from LASS spot analyses.

crystals. The Eu/Eu* of near unity (Fig. 2D) and elevated Zr/Hf (>40; see the Data Repository) provide additional evidence that the quartz monzonites reflect concentration of these minerals (see Bachl et al., 2001; Claiborne et al., 2006).

We suggest a physical model in which a crystal-rich granitic mush lost highly evolved interstitial melt within the optimal crystallinity window (~50%–70%) for melt extraction (Dufek and Bachmann, 2010). The end-member compositions of Afs granite (i.e., frozen rhyolitic liquids) and quartz monzonite (i.e., silicic cumulates) are within this critical crystallinity window in our models (Figs. 2B and 2C). This melt extraction model is independently tested by assessing the mass balance of the Eu anomaly in the three domains of the Huemul pluton (see the Data Repository). The average magnitude of Eu/Eu* in the granite domain (Eu/Eu* = 0.52) is reproduced by extracting Afs granite (0.14) and leaving behind a quartz monzonite (0.93) residue in ~50% proportions. This is self-consistent with our crystallization models and we thus infer a genetic relationship between these Huemul domains and the unmixing of Afs granite melt from a granitic mush to produce residual quartz monzonite. We note that a positive Eu anomaly is not required if feldspar accumulation has occurred from a magma already having Eu/Eu* <1 (Fig. 2D).

Most elements show an apparent compositional gap from 70 to 75 wt% SiO_2 from the Huemul granite to Afs granites (Fig. 2C; see the Data Repository). Compositional gaps at these silica concentrations have been attributed to rhyolite melt segregation from crystalline mush systems in eruptive sequences (Brophy, 1991; Dufek and Bachmann, 2010) and linked subvolcanic intrusion-volcanic pairs (Deering et al., 2016). In addition to these settings, compositional gaps preserved in plutonic systems may also record extraction of rhyolitic melt (e.g., Mahood and Cornejo, 1992).

EVIDENCE FROM ZIRCON GROWTH AND GEOCHEMISTRY

Dispersion of U-Pb zircon dates from individual plutonic hand specimens obviates calculation of singular ages of formation (e.g., Samperton et al., 2015). Thus, interpreting the spectrum of LASS U-Pb zircon dates in each hand specimen is challenging (Fig. 3A; see the Data Repository). However, the range of U-Pb zircon dates reveals that magmas composing the Risco Bayo pluton crystallized and solidified between ca. 7.2 and 6.6 Ma, perhaps as mafic forerunners ~800 k.y. prior to the formation of mush from which Huemul rocks were derived (Fig. 3A). If the three Huemul domains are silicic cumulates, extracted rhyolitic liquids, and mixtures thereof, zircon from each must record crystallization during a period of melt extraction short enough to prevent freezing. That zircon dates of ca. 6.6–6.2 Ma in these domains are indistinguishable from one another is consistent with the melt extraction hypothesis (Fig. 3A).

Eu/Eu* trends in zircon have been interpreted to reflect crystallization from evolving melt undergoing progressive feldspar fractionation or changing oxidation conditions (e.g., Trail et al., 2012). We suggest in this case that feldspar fractionation is the main control of zircon Eu/Eu* in the Huemul pluton. In addition, the flat middle-heavy rare earth element trends (Fig. 2D) imply that Dy/Yb is being controlled by zircon crystallization and not accessory titanite present in Huemul. Thus, the range of Dy/Yb is narrower in Huemul and Eu/Eu* is generally lower than that of Risco Bayo zircon (Fig. 3B), indicative of crystallization from more evolved melt. The compositional variations of zircon from Huemul quartz monzonites and granites are identical in Eu/Eu* and Dy/Yb, regardless of rock type (Fig. 3B). Although cumulate trace element signatures would not be recorded in the minerals, the compositional similarity of zircon from two distinct domains is strong evidence of crystallization from a common magma prior to the formation of contrasts in bulk-rock chemistry. We conclude that accumulation of early crystallized zircon was responsible for enriching Zr in the quartz monzonites (Fig. 2B).

Afs granite zircons display the most evolved trace element signatures and lowest Eu/Eu* of the entire suite (Fig. 3B). Afs granite zircon with Eu/Eu* > 0.1 are within the range of the other two Huemul domains and are interpreted to be the same preaccumulation zircon as in the quartz monzonite, likely from the original mush prior to unmixing. Afs granite zircons with Eu/Eu* > 0.1 are highly evolved (>12,000 ppm Hf; see the Data Repository), indicative of crystallization from rhyolitic melt perhaps concordant with melt extraction. For comparison, distinctions in Eu/Eu* among Risco Bayo zircons imply crystallization of separate magmas (Fig. 3B), consistent with sharp field contacts between incrementally emplaced batches of magma, and suggest that the Huemul pluton did not form by direct fractionation of the mafic Risco Bayo rocks.

CONCLUSIONS

The RBH complex embodies an exceptional plutonic example of fractionated rhyolitic compositions and their complementary silicic cumulate residues. Bulk-rock mass balance suggests that these compositions formed within the optimal window for melt segregation at crystallinities of ~50%–70%. The narrow distribution of LASS U-Pb zircon ages reflects coeval crystallization of large volumes of Huemul Afs granite, within the precision of the technique. Zircon trace element trends link the more evolved Afs granite zircon to the complementary silicic cumulates, supporting the bulk-rock relationships.

The composition and petrology of the Huemul pluton indicates that differentiation via upper crustal crystal-liquid separation within mush zones is an effective mechanism by which potentially eruptible rhyolitic liquid can be generated. The plutonic residue from this process has a silicic cumulate signature that cannot be readily explained as a liquid composition. Despite apparent limits on the global abundance of silicic cumulates gleaned from average volcanic and plutonic differentiation trends (Keller et al., 2015), our results demonstrate that silicic cumulates occur in magmatic arcs like the southern volcanic zone, and that upper crustal melt extraction can produce high-silica granite melt potentially capable of erupting as rhyolite. We emphasize that silicic cumulate rocks may be hidden in global compilations (e.g., Glazner et al., 2015), but can be recognized on a system-specific basis and thus deserve consideration when evaluating the diversity of upper crustal magmatism.

Moreover, while the degree of melt extraction, starting compositions, and partition coefficients all influence detection of silicic cumulates, the direction of complementary unmixing trends is fixed by cumulate mineralogy. The distinctive cumulate signature observed in the Huemul pluton (e.g., enrichment in Ba by a factor of eight relative to extracted liquids) suggests that limited melt extraction alone may be insufficient to obscure the contribution of silicic cumulates to the plutonic record. Additional processes such as retention of extracted melt or cumulate remobilization are required. In situ differentiation via melt extraction is a widely invoked mechanism of rhyolite generation to fuel large silicic eruptions. The same process may also generate high-silica granites, leading to a more universal model of silicic magmatism between the plutonic and volcanic realms.

ACKNOWLEDGMENTS

Supported by National Science Foundation grants EAR-1411779, EAR-1650232, EAR-16502265, and EAR-1650156; University of Wisconsin-Madison Department of Geoscience gift funds; and a Geological Society of America Graduate Research Grant. We thank I. Payacán and F. Gutiérrez for participation in the field. We appreciate constructive reviews by A. Glazner, C. Barnes, L. Claiborne, and J. Miller that improved this manuscript.

REFERENCES CITED

Bachl, C.A., Miller, C.F., Miller, J.S., and Faulds, J.E., 2001, Construction of a pluton: Evidence from an exposed cross section of the Searchlight pluton, Eldorado Mountains, Nevada: Geological Society of America Bulletin, v. 113, p. 1213–1228, doi:10.1130/0016-7606(2001)113<1213:COAPEF>2.0.CO;2.

Bachmann, O., and Bergantz, G.W., 2004, On the origin of crystal-poor rhyolites: Extracted from batholithic crystal mushes: Journal of Petrology, v. 45, p. 1565–1582, doi:10.1093/petrology/egh019.

Bachmann, O., and Huber, C., 2016, Silicic magma reservoirs in the Earth's crust: American Mineralogist, v. 101, p. 2377–2404, doi:10.2138/am-2016-5675.

Brophy, J.G., 1991, Composition gaps, critical crystallinity, and fractional crystallization in orogenic (calc-alkaline) magmatic systems: Contributions to Mineralogy and Petrology, v. 109, p. 173–182, doi:10.1007/BF00306477.

Candela, P.A., 1997, A review of shallow, ore-related granites: Textures, volatiles, and ore metals: Journal of Petrology, v. 38, p. 1619–1633, doi:10.1093/petroj/38.12.1619.

Claiborne, L.L., Miller, C.F., Walker, B.A., Wooden, J.L., Mazdab, F.K., and Bea, F., 2006, Tracking magmatic processes through Zr/Hf ratios in rocks and Hf and Ti zoning in zircons: An example from the Spirit Mountain batholith, Nevada: Mineralogical Magazine, v. 70, p. 517–543, doi:10.1180/0026461067050348.

Deering, C.D., and Bachmann, O., 2010, Trace element indicators of crystal accumulation in silicic igneous rocks: Earth and Planetary Science Letters, v. 297, p. 324–331, doi:10.1016/j.epsl.2010.06.034.

Deering, C.D., Keller, B., Schoene, B., Bachmann, O., Beane, R., and Ovtcharova, M., 2016, Zircon record of the plutonic-volcanic connection and protracted rhyolite melt evolution: Geology, v. 44, p. 267–270, doi:10.1130/G37539.1.

Drake, R.E., 1976, Chronology of Cenozoic igneous and tectonic events in the central Chilean Andes—Latitudes 35°30′ to 36°S: Journal of Volcanology and Geothermal Research, v. 1, p. 265–284, doi:10.1016/0377-0273(76)90011-1.

Dufek, J., and Bachmann, O., 2010, Quantum magmatism: Magmatic compositional gaps generated by melt-crystal dynamics: Geology, v. 38, p. 687–690, doi:10.1130/G30831.1.

Gelman, S.E., Deering, C.D., Bachmann, O., Huber, C., and Gutiérrez, F.J., 2014, Identifying the crystal graveyards remaining after large silicic eruptions: Earth and Planetary Science Letters, v. 403, p. 299–306, doi:10.1016/j.epsl.2014.07.005.

Glazner, A.F., Coleman, D.S., and Mills, R.D., 2015, The volcanic-plutonic connection, *in* Breitkreuz, C., and Rocchi, S., eds., Physical geology of shallow magmatic systems: Dykes, sills and laccoliths: Advances in Volcanology: New York, Springer International Publishing, p. 1–22.

Gualda, G.A.R., Ghiorso, M.S., 2014, Phase-equilibrium geobarometers for silicic rocks based on rhyolite-MELTS. Part 1: Principles, procedures, and evaluation of the method: Contributions to Mineralogy and Petrology, v. 168, p. 1–17, doi:10.1007/s00410-014-1033-3.

Hildreth, W., 2004, Volcanological perspectives on Long Valley, Mammoth Mountain, and Mono Craters: Several contiguous but discrete systems: Journal of Volcanology and Geothermal Research, v. 136, p. 169–198, doi:10.1016/j.jvolgeores.2004.05.019.

Keller, C.B., Schoene, B., Barboni, M., Samperton, K.M., and Husson, J.M., 2015, Volcanic-plutonic parity and the differentiation of the continental crust: Nature, v. 523, p. 301–307, doi:10.1038/nature14584.

Kylander-Clark, A.R.C., Hacker, B.R., and Cottle, J.M., 2013, Laser-ablation split-stream ICP petrochronology: Chemical Geology, v. 345, p. 99–112, doi:10.1016/j.chemgeo.2013.02.019.

Lee, C.T.A., and Morton, D.M., 2015, High silica granites: Terminal porosity and crystal settling in shallow magma chambers: Earth and Planetary Science Letters, v. 409, p. 23–31, doi:10.1016/j.epsl.2014.10.040.

Lundstrom, C.C., and Glazner, A.F., 2016, Silicic magmatism and the volcanic-plutonic connection: Elements, v. 12, p. 91–96, doi:10.2113/gselements.12.2.91.

Mahood, G.A., and Cornejo, P.C., 1992, Evidence for ascent of differentiated liquids in a silicic magma chamber found in a granitic pluton: Royal Society of Edinburgh Transactions, Earth Sciences, v. 83, p. 63–69, doi:10.1017/S0263593300007756.

Nelson, S.T., Davidson, J.P., Heizler, M.T., and Kowallis, B.J., 1999, Tertiary tectonic history of the southern Andes: The subvolcanic sequence to the Tatara–San Pedro volcanic complex, lat 36°S: Geological Society of America Bulletin, v. 111, p. 1387–1404, doi:10.1130/0016-7606(1999)111<1387:TTHOTS>2.3.CO;2.

Samperton, K., Schoene, B., Cottle, J.M., Keller, C.B., Crowley, J.L., and Schmitz, M., 2015, Magma emplacement, differentiation and cooling in the middle crust: Integrated zircon geochronological-geochemical constraints from the Bergell Intrusion, Central Alps: Chemical Geology, v. 417, p. 322–340, doi:10.1016/j.chemgeo.2015.10.024.

Singer, B.S., Thompson, R.A., Dungan, M.A., Feeley, T.C., Nelson, S.T., Pickens, J.C., Brown, L.L., Wulff, A.W., Davidson, J.P., and Metzger, J., 1997, Volcanism and erosion during the past 930 k.y. at the Tatara–San Pedro complex, Chilean Andes: Geological Society of America Bulletin, v. 109, p. 127–142, doi:10.1130/0016-7606(1997)109<0127.

Trail, D., Watson, E.B., and Tailby, N.D., 2012, Ce and Eu anomalies in zircon as proxies for the oxidation state of magmas: Geochimica et Cosmochimica Acta, v. 97, p. 70–87, doi:10.1016/j.gca.2012.08.032.

Vernon, R.H., and Collins, W.J., 2011, Structural criteria for identifying granitic cumulates: Journal of Geology, v. 119, p. 127–142, doi:10.1086/658198.

Wager, L.R., and Brown, G.M., 1968, Layered igneous rocks: San Francisco, California, W.H Freeman and Company, 587 p.

Manuscript received 21 March 2017
Revised manuscript received 25 May 2017
Manuscript accepted 26 May 2017

Printed in USA